Inorg. Chem. **2002**, *41*, 3110–3120

Steric Control of Substituted Phenoxide Ligands on Product Structures of Uranyl Aryloxide Complexes

Marianne P. Wilkerson,[†,‡] Carol J. Burns,*[,†] David E. Morris,[†] Robert T. Paine,[‡] and Brian L. Scott[†]

The Chemistry Division, Los Alamos National Laboratory, Los Alamos, New Mexico 87545, and Department of Chemistry, University of New Mexico, Albuquerque, New Mexico 87131

Received October 18, 2001

A series of uranyl aryloxide complexes has been prepared via metathesis reactions between $[UO_2Cl_2(THF)_2]_2$ and di-*ortho*-substituted phenoxides. Reaction of 4 equiv of KO-2,6-^{t}Bu$_2$C$_6$H$_3$ with $[UO_2Cl_2(THF)_2]_2$ in THF produces the dark red uranyl compound, UO_2(O-2,6-^{t}Bu$_2$C$_6$H$_3$)$_2$(THF)$_2$·THF, **1**. Single-crystal X-ray diffraction analysis of **1** reveals a monomer in which the uranium is coordinated in a pseudooctahedral fashion by two apical oxo groups, two *cis*-aryloxides, and two THF ligands. A similar product is prepared by reaction of KO-2,6-Ph$_2$C$_6$H$_3$ with $[UO_2Cl_2(THF)_2]_2$ in THF. Single-crystal X-ray diffraction analysis of this compound reveals it to be the *trans*-monomer UO_2(O-2,6-Ph$_2$C$_6$H$_3$)$_2$(THF)$_2$, **2**. Dimeric structures result from the reactions of $[UO_2Cl_2(THF)_2]_2$ with less sterically imposing aryloxide salts, KO-2,6-Cl$_2$C$_6$H$_3$ or KO-2,6-Me$_2$C$_6$H$_3$. Single-crystal X-ray diffraction analyses of $[UO_2$(O-2,6-Cl$_2$C$_6$H$_3$)$_2$(THF)$_2]_2$, **3**, and $[UO_2$Cl(O-2,6-Me$_2$C$_6$H$_3$)(THF)$_2]_2$, **4**, reveal similar structures in which each U atom is coordinated by seven ligands in a pseudopentagonal bipyramidal fashion. Coordinated to each uranium are two apical oxo groups and five equatorial ligands (**3**, one terminal phenoxide, two bridging phenoxides, and two nonadjacent terminal THF ligands; **4**, one terminal chloride, two bridging phenoxides, and two nonadjacent terminal THF ligands). Apparently, the phenoxide ligand steric features exert a greater influence on the solid-state structures than the electronic properties of the substituents. Emission spectroscopy has been utilized to investigate the molecularity and electronic structure of these compounds. For example, luminescence spectra taken at liquid nitrogen temperature allow for a determination of the dependence of the molecular aggregation of **3** on the molecular concentration. Electronic and vibrational spectroscopic measurements have been analyzed to examine trends in emission energies and stretching frequencies. However, comparison of the data for compounds **1**–**4** reveals that the innate electron-donating capacity of phenoxide ligands is only subtly manifest in either the electronic or vibrational energy distributions within these molecules.

Introduction

Molecular structures of uranium compounds containing the uranyl cation UO_2^{2+} are the most common class reported for this element.[1] The majority of these compounds have been prepared in protic solutions,[2] and they typically produce aggregates,[3] in which uranyl groups lie parallel to one another in dimers,[4] trimers,[5] tetramers,[6] hexamers,[7] chains,[8] and even channels or helices.[9] Aggregation of the uranyl ions is achieved through bridging ligands that are coordinated in the equatorial plane of UO_2^{2+}. However, these structures do not provide any evidence for Lewis base behavior of the uranyl oxo groups, as is seen for transition metal oxo analogues.[10]

More recently, it has been demonstrated that the generation of uranyl compounds with more electron-rich ligands in nonaqueous media can enhance the basicity of the oxo

* Author to whom correspondence should be addressed. Fax: (505) 665-4355. E-mail: cjb@lanl.gov.

† Los Alamos National Laboratory.

‡ University of New Mexico.

(1) (a) Cotton, S. *Lanthanides and Actinides*; Macmillan Education Ltd.: London, 1991; Chapter 3. (b) Greenwood, N. N.; Earnshaw, A. *Chemistry of the Elements*; Pergamon Press: New York, 1984; Chapter 31.

(2) Weigel, F. In *The Chemistry of the Actinide Elements*; Katz, J. J., Seaborg, G. T., Morss, L. R., Eds.; Chapman and Hall: New York, 1986; Vol. 1.

(3) (a) Wells, A. F. In *Structural Inorganic Chemistry*; Clarendon Press: Oxford, 1995; Chapter 28. (b) Burns, J. H. In *The Chemistry of the Actinide Elements*; Katz, J. J., Seaborg, G. T., Morss, L. R., Eds.; Chapman and Hall: New York, 1986; Vol. 2. (c) Denning, R. G. In *Gmelin Handbook of Inorganic Chemistry*; Buschbeck., K.-C., Keller, C., Eds.; Springer-Verlag: Heidelberg, Germany, 1983; Vol. A6, p 31.

10.1021/ic011080q CCC: $22.00
Published on Web 05/24/2002

group.[11] For example, the reaction of $[UO_2Cl_2(THF)_2]_2$[12] with alkoxide ligands can give rise to aggregates containing bridging oxo groups. In the extreme, complexes resulting from ligand redistribution have been isolated, which presumably form from such oxo-bridged intermediates. Evidence for these proposed intermediates lies in the bonding mode of an isolated tetrameric compound in which uranyl groups are connected via bridging uranyl oxo ligands.[11b]

One question that arises is how sensitive this oxo basicity is to variation in the steric versus electronic characteristics of the alkoxide groups. This question has led us to examine a range of binary uranyl aryloxide systems. While there is a paucity of structurally characterized examples of uranyl aryloxides reported in the literature,[13] we have generated a variety of these new species by utilizing metathesis and alcoholysis routes. Although some variability is observed in the molecularity of the products, the phenoxide complexes are not found to support redistribution. Rather, simple binary products are isolated in which the molecularity (monomer vs dimer) appears to be determined principally by the steric constraints imposed by the associated ligand.

Experimental Section

General Information. Standard inert-atmosphere techniques were used for the manipulation of all reactions.[14] ^{1}H-NMR spectra (300 MHz) were measured on a Varian UNITYplus-300 spectrometer. The chemical shifts are reported relative to the protio impurity of the deuterated solvent (C_6D_6, $\delta = 7.15$; toluene-d_8, $\delta = 2.08$). All spectra were recorded at 298 K unless indicated otherwise. The samples were dissolved in a deuterated lock solvent and then contained in sealed Teflon liners, which were then placed in 5 mm tubes. Infrared spectra were recorded on a Magna-IR System 750 spectrometer from Nujol mulls. Elemental analyses were performed in our laboratories on a Perkin-Elmer 2400 CHN analyzer. The samples were prepared and sealed in tin capsules in the inert-atmosphere box prior to combustion.

Luminescence data were obtained on a SPEX Industries Fluorolog 2 system consisting of a model 1681 single-stage 0.22 m excitation monochromator and a model 1680 two-stage emission monochromator. All gratings were 1200 groove/mm. The emitted light was detected by a thermoelectrically cooled Hamamatsu model R928 photomultiplier tube and processed with photon-counting electronics. Continuous-wave spectra were collected using the output from a 450 W Xe arc lamp. Time-resolved data were collected using the output from a hydrogen flash lamp controlled by a SPEX model 1934D phosphorimeter attachment. Samples were contained in sealed glass capillary tubes that were loaded under an inert atmosphere. Data were obtained at approximately liquid N_2 temperature using a simple insertion dewar and front-face collection optics. Integration times were 1−4 s per wavelength increment,

(4) (a) Beer, P. D.; Drew, M. G. B.; Hesek, D.; Kan, M.; Nicholson, G.; Schmitt, P.; Sheen, P. D.; Williams, G. *J. Chem. Soc., Dalton Trans.* **1998**, 2783. (b) Hämäläinen, R.; Turpeinen, U.; Mutikainen, I. *Acta Crystallogr., Sect. C* **1996**, *52*, 16. (c) Rudkevich, D. M.; Verboom, W.; Brzozka, Z.; Palys, M. J.; Stauthamer, W. P. R. V.; van Hummel, G. J.; Franken, S. M.; Harkema, S.; Engbersen, J. F. J.; Reinhoudt, D. N. *J. Am. Chem. Soc.* **1994**, *116*, 4341. (d) Cragg, P. J.; Bott, S. G.; Atwood, J. L. *Lanthanide Actinide Res.* **1988**, *2*, 265. (e) Alcock, N. W.; Flanders, D. J. *Acta Crystallogr., Sect. C* **1987**, *43*, 1267. (f) Govindarajan, S.; Patil, K. C.; Poojary, M. D.; Manohar, H. *Inorg. Chim. Acta* **1986**, *120*, 103. (g) Charpin, P.; Folcher, G.; Lance, M.; Nierlich, M.; Vigner, D. *Acta Crystallogr., Sect. C* **1985**, *41*, 1302. (h) Viossat, B.; Dung, N.-H.; Soye, C. *Acta Crystallogr., Sect. C* **1983**, *39*, 573. (i) Bombieri, G.; Degetto, S.; Forsellini, E.; Marangoni, G. *Cryst. Struct. Commun.* **1977**, *6*, 115. (j) Perrin, A. *Acta Crystallogr., Sect. B* **1976**, *32*, 1658. (k) Nassimbeni, L. R.; Rodgers, A. L.; Haigh, J. M. *Inorg. Chim. Acta* **1976**, *20*, 149. (l) Åberg, M. *Acta Chem. Scand.* **1969**, *23*, 791.

(5) (a) Silverwood, P. R.; Collison, D.; Livens, F. R.; Beddoes, R. L.; Taylor, R. J. *J. Alloys Compd.* **1998**, *271*−*273*, 180. (b) Allen, P. G.; Bucher, J. J.; Clark, D. L.; Edelstein, N. M.; Ekberg, S. A.; Gohdes, J. W.; Hudson, E. A.; Kaltsoyannis, N.; Lukens, W. W.; Neu, M. P.; Palmer, P. D.; Reich, T.; Shuh, D. K.; Tait, C. D.; Zwick, B. D. *Inorg. Chem.* **1995**, *34*, 4797. (c) Cousson, A.; Nectoux, F.; Pagès, M.; Rizkalla, E. N. *Radiochim. Acta* **1993**, *61*, 177. (d) Lintvedt, R. L.; Heeg, M. J.; Ahmad, N.; Glick, M. D. *Inorg. Chem.* **1982**, *21*, 2350. (e) Åberg, M. *Acta Chem. Scand.* **1978**, *A32*, 101.

(6) (a) Turpeinen, U.; Hämäläinen, R.; Mutikainen, I.; Orama, O. *Acta Crystallogr., Sect. C* **1996**, *52*, 1169. (b) Åberg, M. *Acta Chem. Scand.* **1976**, *A30*, 507. (c) Åberg, M. *Acta Chem. Scand.* **1971**, *25*, 368.

(7) Charpin, P.; Lance, M.; Nierlich, M.; Vigner, D.; Livet, J.; Musikas, C. *Acta Crystallogr., Sect. C* **1986**, *42*, 1691.

(8) (a) Grohol, D.; Gingl, F.; Clearfield, A. *Inorg. Chem.* **1999**, *38*, 751. (b) Francis, R. J.; Drewitt, M. J.; Halasyamani, P. S.; Ranganathachar, C.; O'Hare, D.; Clegg, W.; Teat, S. J. *Chem. Commun*. **1998**, 279. (c) Grohol, D.; Clearfield, A. *J. Am. Chem. Soc.* **1997**, *119*, 4662. (d) Grohol, D.; Subramanian, M. A.; Poojary, D. M.; Clearfeld, A. *Inorg. Chim. Acta* **1996**, *35*, 5264. (e) Russell, A. A.; Meline, R. L.; Duelser, E. N.; Paine, R. T. *Inorg. Chim. Acta* **1995**, *231*, 1. (f) Thuéry, P.; Keller, N.; Lance, M.; Vigner, J.-D.; Nierlich, M. *Acta Crystallogr., Sect. C* **1995**, *51*, 1526. (g) Alcock, N. W.; Kemp, T. J.; Leciejewicz, J. *Inorg. Chim. Acta* **1993**, *203*, 81. (h) Alcock, N. W.; Kemp, T. J.; Leciejewicz, J. *Inorg. Chim. Acta* **1991**, *184*, 203. (i) Rogers, R. D.; Bond, A. H.; Hipple, W. G.; Rollins, A. N.; Henry, R. F. *Inorg. Chem.* **1991**, *30*, 2671. (j) Nierlich, M.; Iroulart, G.; Vigner, D.; Keller, N.; Lance, M. *Acta Crystallogr., Sect. C* **1990**, *46*, 2459. (k) Britel, A.; Wozniak, M.; Boivin, J. C.; Nowogrocki, G.; Thomas, D. *Acta Crystallogr., Sect. C* **1986**, *42*, 1502. (l) Burns, J. H. *Inorg. Chem.* **1983**, *22*, 1174. (m) Toivonen, J.; Niinistö, L. *Inorg. Chem.* **1983**, *22*, 1557. (n) Bombieri, G.; Benetollo, F.; Rojas, R. M.; De Paz, M. L.; Del Pra, A. *Inorg. Chim. Acta* **1982**, *61*, 149. (o) Bombieri, G.; Benetollo, F.; Rojas, R. M.; De Paz, M. L. *J. Inorg. Nucl. Chem.* **1981**, *43*, 3203. (p) Mentzen, B. F.; Sautereau, H. *Acta Crystallogr., Sect. B* **1980**, *36*, 2051. (q) Ruben, H.; Spencer, B.; Templeton, D. H.; Zalkin, A. *Inorg. Chem.* **1980**, *19*, 776.

(9) (a) Aranda, M. A. G.; Cabeza, A.; Bruque, S.; Poojary, D. M.; Clearfield, A. *Inorg. Chem.* **1998**, *37*, 1827. (b) Poojary, D. M.; Cabeza, A.; Aranda, M. A. G.; Bruque, S.; Clearfield, A. *Inorg. Chem.* **1996**, *35*, 1468. (c) Poojary, D. M.; Grohol, D.; Clearfield, A. *Angew. Chem., Int. Ed. Engl.* **1995**, *34*, 1508. (d) Doyle, G. A.; Goodgame, D. M. L.; Sinden, A.; Williams, D. J. *J. Chem. Soc., Chem. Commun.* **1993**, 1170. (e) Immirzi, A.; Bombieri, G.; Degetto, S.; Marangoni, G. *Acta Crystallogr., Sect. B* **1975**, *31*, 1023.

(10) (a) Norquist, A. J.; Stern, C. L.; Poeppelmeier, K. R. *Inorg. Chem.* **1999**, *38*, 3448. (b) Hotzelmann, R.; Wieghardt, K.; Ensling, J.; Romstedt, H.; Gütlich, P.; Bill, E.; Flörke, U.; Haupt, H.-J. *J. Am. Chem. Soc.* **1992**, *114*, 9470. (c) Housmekerides, C. E.; Romage, D. L.; Kretz, C. M.; Shontz, J. T.; Pilato, R. S.; Geoffroy, G. L.; Rheingold, A. L.; Haggerty, B. S. *Inorg. Chem.* **1992**, *31*, 4453. (d) Rau, M. S.; Kretz, C. M.; Mercando, L. A.; Geoffroy, G. L.; Rheingold, A. L. *J. Am. Chem. Soc.* **1991**, *113*, 7420. (e) Pilato, R. S.; Rubin, D.; Geoffroy, G. L.; Rheingold, A. L. *Inorg. Chem.* **1990**, *29*, 1986. (f) Schreiber, P.; Wieghardt, K.; Nuber, B.; Weiss, J. *Polyhedron* **1989**, *8*, 1675. (g) West, B. O. *Polyhedron* **1989**, *8*, 219. (h) Yang, C.-H.; Ladd, J. A.; Goedken, V. L. *J. Coord. Chem.* **1988**, *19*, 235. (i) Rybak, W. K.; Ziółkowski, J. J. *J. Mol. Catal.* **1987**, *42*, 347. (j) Bèlanger, S.; Beauchamp, A. L. *Inorg. Chem.* **1996**, *35*, 7836. (k) Mayer, J. M. *Polyhedron* **1995**, *14*, 3273. (l) Herrmann, W. A.; Fischer, R. A.; Amslinger, W.; Herdtweck, E. *J. Organomet. Chem.* **1989**, *362*, 333.

(11) (a) Wilkerson, M. P.; Burns, C. J.; Morris, D. E.; Paine, R. T.; Scott, B. L., manuscript in preparation. (b) Wilkerson, M. P.; Burns, C. J.; Dewey, H. J.; Martin, J. M.; Morris, D. E.; Paine, R. T.; Scott, B. L. *Inorg. Chem.* **2000**, *39*, 5277. (c) Burns, C. J.; Sattelberger, A. P. *Inorg. Chem.* **1988**, *27*, 3692.

(12) (a) Wilkerson, M. P.; Burns, C. J.; Paine, R. T.; Scott, B. L. *Inorg. Chem.* **1999**, *38*, 4156. (b) Charpin, P.; Lance, M.; Nierlich, M.; Vigner, D.; Baudin, C. *Acta Crystallogr., Sect. C* **1987**, *43*, 1832. (c) Rogers, R. D.; Green, L. M.; Benning, M. M. *Lanthanide Actinide Res.* **1986**, *1*, 185.

(13) Barnhart, D. M.; Burns, C. J.; Sauer, N. N.; Watkin, J. G. *Inorg. Chem.* **1995**, *34*, 4079.

(14) Shriver, D. F.; Drezdzon, M. A. *The Manipulation of Air-Sensitive Compounds*, 2nd ed.; Wiley-Interscience: New York, 1986.

and two to four spectra were typically averaged to derive each final spectrum. The emission data reported here have not been corrected for monochromator or detector response.

To extract vibrational data from the vibronically resolved emission spectra, the wavelengths were first transformed to the energy (cm^{-1}) domain. The data were fit to Gaussian model equations based upon empirical observations of the peaks. Gaussian fits were determined using a standard nonlinear least-squares, curve-fitting routing available on IGOR[15] software running on a Macintosh platform.

The Raman spectroscopy was carried out using a microscope system or a macroscopic FT-Raman system. The microscope system consists of a Zeiss Axiovert 135TV inverted microscope equipped with a 20× objective (numerical aperture = 0.40). Raman scattered light was collected through a Kaiser Optical Systems Holospec holographic spectrometer equipped with a 752 nm holographic grating and imaged on a liquid nitrogen cooled Photometrics CS210 CCD with a 514 × 514 pixel chip. The spectrometer/CCD system was calibrated using the Raman spectrum of toluene. Samples were contained in sealed glass capillary tubes loaded under an inert atmosphere. All spectra were acquired with ∼15 mW (measured at the sample) at 752 nm. Four to ten sets of spectra with 30−60 s integration times were collected and averaged. The FT-Raman system is a Nicolet model 960 FT-Raman spectrometer attached to a Nicolet model 560 Magna-IR with an extended XT-KBr beam splitter and 180° sampling geometry. The excitation source is the 1064 nm light from a YVO_4:Nd^{3+} laser. A 0.4 neutral density filter was used to decrease the laser power toward the sample to ∼100 mW. The interferograms were detected with an InGaAs detector operated at room temperature. An average of 256 scans at 8 cm^{-1} of resolution was taken to give each spectrum.

Materials. Anhydrous uranyl chloride bis(tetrahydrofuran), $[UO_2Cl_2(THF)_2]_2$,[12a] and $UO_2[N(SiMe_3)_2]_2(THF)_2$[13,16] were prepared by literature methods. Potassium hydride, HO-2,6-^{t}Bu$_2$C$_6$H$_3$, HO-2,6-Ph$_2$C$_6$H$_3$, HO-2,6-Cl$_2$C$_6$H$_3$, and HO-2,6-Me$_2$C$_6$H$_3$ were purchased from Aldrich. The phenols were purified by sublimation. Reagents KO-2,6-^{t}Bu$_2$C$_6$H$_3$, KO-2,6-Ph$_2$C$_6$H$_3$, KO-2,6-Cl$_2$C$_6$H$_3$, and KO-2,6-Me$_2$C$_6$H$_3$ were prepared from the appropriate dry phenol and KH in tetrahydrofuran at room temperature, and were dried in vacuo prior to use. Solvents were rigorously dried by standard methods.[14]

Synthesis and Characterization. UO_2(O-2,6-^{t}Bu$_2$C$_6$H$_3$)$_2$(THF)$_2$·THF (1). KO-2,6-^{t}Bu$_2$C$_6$H$_3$ (2.02 g, 8.26 mmol) was dissolved in THF (20 mL), and this solution was added to a slurry of $[UO_2Cl_2(THF)_2]_2$ (2.00 g, 2.06 mmol) in THF (50 mL). The solution was stirred for ∼4 h and then filtered over Celite. The filtrate was concentrated to ∼5 mL, layered with ∼5 mL of hexane, and cooled to −30 °C, yielding dark red blocks (3.05 g, 3.54 mmol, 86%). ^{1}H-NMR (C_6D_6, δ): 7.74 (2H, d, $^3J_{HH}$ = 8 Hz, *m*-OAr), 6.84 (1H, t, $^3J_{HH}$ = 8 Hz, *p*-OAr), 4.24 (4H, m, α-THF), 1.80 (18H, s, ^{t}Bu), 1.35 (4H, m, β-THF). IR (Nujol): 1559m, 1399s, 1310w, 1300w, 1260s, 1244s, 1226s, 1212w, 1199w, 1152w, 1128w, 1117m, 1102m, 1054m, 1038m, 952w, 915m, 896s, 887m, 858s, 819s, 805s, 797s, 752s, 750s cm^{-1}. Anal. Calcd for $C_{38}H_{62}O_{6.5}U$: C, 53.02; H, 7.26. Found: C, 51.96; H, 7.43.

UO_2(O-2,6-Ph$_2$C$_6$H$_3$)$_2$(THF)$_2$ (2). Method A. KO-2,6-Ph$_2$C$_6$H$_3$ (0.59 g, 2.1 mmol) was dissolved in THF (20 mL), and this solution was added to a slurry of $[UO_2Cl_2(THF)_2]_2$ (0.50 g, 0.52 mmol) in THF (50 mL). The solution was stirred for ∼3 h, during which time an orange powder formed. The solvent was removed under a vacuum, and the product was washed with THF three times and dried under a vacuum (0.80 g, 0.88 mmol, 86%). **Method B.** HO-2,6-Ph$_2$C$_6$H$_3$ (0.06 g, 0.2 mmol) was dissolved in THF (5 mL), and this solution was added to a solution of $UO_2[N(SiMe_3)_2]_2(THF)_2$ (0.09 g, 0.1 mmol) in THF (5 mL). The solution was stirred overnight, during which time an orange powder formed. The powder was filtered, washed three times with hexane, and dried under a vacuum (0.08 g, 0.09 mmol, 90%). The compound was too insoluble in hydrocarbon solvents to obtain solution NMR data. IR (Nujol): 1419w, 1407s, 1399w, 1394w, 1310m, 1287w, 1279m, 1259s, 1086m, 1071m, 1056w, 972w, 918w, 897s, 885m, 862s, 853s, 800s, 761s, 755s, 705s, 689m cm^{-1}. Anal. Calcd for $C_{44}H_{42}O_6U$: C, 58.41; H, 4.68. Found: C, 58.24; H, 4.75.

$[UO_2$(O-2,6-Cl$_2$C$_6$H$_3$)$_2$(THF)$_2]_2$ (3). KO-2,6-Cl$_2$C$_6$H$_3$ (0.41 g, 2.0 mmol) was dissolved in THF (20 mL), and this solution was added to a slurry of $[UO_2Cl_2(THF)_2]_2$ (0.50 g, 0.52 mmol) in THF (20 mL). The solution was stirred for ∼4 h and then filtered over Celite. The filtrate was concentrated to ∼5 mL, layered with ∼5 mL of hexane, and cooled to −30 °C, yielding orange needles (0.33 g, 0.22 mmol, 44%). ^{1}H-NMR (C_6D_6, δ): 7.36 (2H, d, $^3J_{HH}$ = 8 Hz, *m*-OAr), 6.25 (1H, t, $^3J_{HH}$ = 8 Hz, *p*-OAr), 4.29 (4H, m, α-THF), 1.45 (4H, m, β-THF). IR (Nujol/KBr): 1572m, 1317m, 1300s, 1281w, 1255s, 1197m, 1170m, 1149w, 1141w, 1098w, 1089w, 1017s, 937s, 887s, 861m, 842s, 805sh, 776s, 761, 741s cm^{-1}. Anal. Calcd for $C_{40}H_{44}Cl_8O_{12}U_2$: C, 32.54; H, 3.00. Found: C, 32.18; H, 3.31.

$[UO_2$Cl(O-2,6-Me$_2$C$_6$H$_3$)(THF)$_2]_2$ (4). KO-2,6-Me$_2$C$_6$H$_3$ (0.17 g, 1.0 mmol) was dissolved in THF (10 mL), and this solution was added to a slurry of $[UO_2Cl_2(THF)_2]_2$ (0.50 g, 0.52 mmol) and THF (40 mL). The solution was stirred for ∼2 h and then filtered over Celite. The filtrate was concentrated to ∼5 mL, layered with ∼5 mL of hexane, and cooled to −30 °C, yielding dark red blocks (0.39 g, 0.34 mmol, 68%). The compound was too insoluble in hydrocarbon solvents to obtain solution NMR data. IR (Nujol/KBr): 1305w, 1258w, 1198sh, 1186s, 1091m, 1075w, 1014s, 959sh, 942s, 931s, 876w, 863m, 836s, 774m, 765m, 752m, 745m, 678m cm^{-1}. Anal. Calcd for $C_{32}H_{50}Cl_2O_{10}U_2$: C, 33.67; H, 4.41. Found: C, 31.12; H, 4.37.

Crystallographic Measurements and Structure Solution. Crystals of **1** were obtained from toluene solution. Crystallization of **2** from a tetrahydrofuran solution of $UO_2[N(SiMe_3)_2]_2(THF)_2$ layered with a hexane solution of 2 equiv of HO-2,6-Ph$_2$C$_6$H$_3$ at 25 °C resulted in the formation of garnet blocks. Crystals of **3** and **4** were obtained as described above. In each case, a single crystal was mounted onto a glass fiber from a pool of mineral oil under an argon gas flow. The crystal was then immediately placed under a liquid nitrogen vapor stream on a Siemens P4 diffractometer (**1**−**3**). The crystal of **4** was placed on a Siemens P4/CCD. Lattice determination and data collection for **1**−**3** were carried out using XSCANS 2.10b software,[17] and Lorentz and polarization (L−p) corrections, data processing, and structure solution were performed using SHELXTL 4.2/360.[17] For **4**, data collection, initial indexing, and cell refinement was handled using SMART 4.210.[17] Frame integration, L−p corrections, and final cell parameter calculation were performed using SAINT 4.05.[17] Structure solution was performed using SHELXTL 5.10.[17] The refinement, graphics, and creation of publication tables were carried out using SHELXTL 5.10 for all structures. Empirical absorption corrections (XEMP for **1**−**3**)[17] and SADABS[18] (**4**) were applied to all data. Decay of reflection intensity was not observed for any of the samples.

(15) *IGOR Pro 3.12*; WaveMetrics, Inc.,: Lake Oswego, OR.
(16) Andersen, R. A. *Inorg. Chem.* **1979**, *18*, 209.
(17) XSCANS, SHELXTL, XEMPT, SAINT, SMART, and Gemini are products of Bruker AXS, Inc. (formerly Siemens), Madison, WI.

Table 1. Crystal and Structure Refinement Data for UO_2(O-2,6-^{t}Bu$_2$C$_6$H$_3$)$_2$(THF)$_2$·THF (**1**), UO_2(O-2,6-Ph$_2$C$_6$H$_3$)$_2$(THF)$_2$ (**2**), and [UO_2(O-2,6-Cl$_2$C$_6$H$_3$)$_2$(THF)$_2$]$_2$ (**3**)

	1	**2**	**3**
empirical formula	$C_{40}H_{66}O_7U$	$C_{88}H_{84}O_{12}U_2$	$C_{40}H_{44}Cl_8O_{12}U_2$
fw	896.96	1809.6	1476.4
temp, °C	−70	−70	−70
wavelength, Å	0.71073	0.71073	0.71073
space group	$P\bar{1}$	$P2_1$	$R\bar{3}$
a, Å	11.252(2)	15.385(2)	31.836(5)
b, Å	14.658(2)	18.443(1)	31.836(5)
c, Å	14.662(2)	12.773(3)	13.690(3)
α, deg	62.51(1)	−	−
β, deg	79.82(1)	89.987(13)	−
γ, deg	70.25(1)	−	−
volume, Å^3	2018.4(5)	3624(1)	12 016(4)
Z	2	2	9
d_{calc}, g cm^{-3}	1.417	1.658	1.836
abs coeff, mm^{-1}	4.061	4.299	6.509
transm coeff	0.36−0.72	0.12−0.28	0.20−0.68
final R^a indices [$I > 2\sigma(I)$]: R1, wR2	0.057, 0.118	0.045, 0.114	0.050, 0.092

[a] Based on F_o^2. R1 = $\Sigma||F_o| - |F_c||/\Sigma|F_o|$; wR2 = $[\Sigma w(F_o^2 - F_c^2)^2/\Sigma w(F_o^2)^2]^{1/2}$, and $w = 1/[\sigma^2(F_o^2) + (xP)^2]$.

All structures were solved using direct methods and difference Fourier techniques. All hydrogen atom positions were idealized and rode on the atoms to which they were attached. The refinements of structures **1** and **3** proceeded in normal fashion and converged with all non-hydrogen atoms refined anisotropically. (A toluene lattice molecule was found for **1**, and was refined isotropically without hydrogen atoms.) Additional structure solution and refinement parameters for **1**−**3** are listed in Table 1.

The structure solution and refinement of **2** was problematic. The R_{int} was 0.031 and 0.038 for the 2/*m* and *mmm* Laue groups, respectively. The structure solution in $P2_12_12_1$ refined to $R_1(I > 2\sigma) \sim 0.17$, but failed to converge. Anomalous bond distances and angles were also present. A solution in the monoclinic space group, $P2_1$, was pursued at this juncture. The structure was refined as a pseudomerohedral twin, with a 55(4)% component. Due to a low number of data, the structure was refined with anisotropic temperature factors on the uranium and oxygen atoms only. This refinement converged to $R_1(I > 2\sigma) = 0.045$, and resulted in more chemically reasonable bond distances and angles than the refinement in $P2_12_12_1$. The symmetry checking program ADDSYM,[19] when run on the $P2_1$ solution, revealed pseudo-2_1 axes along *a* and *b*. However, the systematic absences showed weak violations for these symmetry elements. These violations, coupled with the better refinement in $P2_1$, resulted in the choice of the lower symmetry space group. Hydrogen atom positions were not included in the final model.

The structure of **4** was solved in space group $P2_1/n$, but only refined to $R_1(I > 2\sigma) = 0.19$. The structure also had numerous large residual peaks scattered throughout the unit cell (maximum = 7.5 e Å^{-3}). The program Gemini[20] was used to integrate the data using two orientation matrixes corresponding to a rotation twin. The structure was then refined using several batch scale factors to model the intensity as a function of varying overlap of the twinned reflections. This twin refinement resulted in $R_1(I > 2\sigma) = 0.116$, but several large residual peaks were still present. Several bond distance restraints were used on the THF ligands. The final refinement included anisotropic temperature factors on uranium and chloride atoms only. Hydrogen atoms were not included in the final model. The connectivity is shown in Figure 4. Additional structure solution and refinement parameters for **4** may be found in the Supporting Information.

Results and Discussion

Synthesis and Structural Characterization. The starting material, [$UO_2Cl_2(THF)_2$]$_2$,[12a] is a convenient entry into the chemistry of uranyl alkoxide compounds. Limitations exist on the range of soluble phenoxide complexes that may be isolated, however. Previous reports have suggested that uranyl monosubstituted phenoxide complexes are polymeric, based upon elemental analysis and infrared data.[21] Our attempts with either unsubstituted phenoxides or *meta*- and/or *para*-substituted phenoxides similarly suggest the formation of polymeric products, yielding only insoluble amorphous powders. However, it is possible to obtain crystalline uranyl products upon coordination of di-*ortho*-substituted phenoxides. To systematically probe the steric and electronic effects of the phenoxides on uranyl, we have chosen a series of di-*ortho*-substituted phenoxide ligands with *tert*-butyl, phenyl, chloro, and methyl substituents.

The addition of 4 equiv of KO-2,6-^{t}Bu$_2$C$_6$H$_3$ to a slurry of [$UO_2Cl_2(THF)_2$]$_2$ at room temperature resulted in an immediate color change from yellow to red. Low-temperature crystallization from a THF/hexane solution allowed for the isolation of dark red blocks of UO_2(O-2,6-^{t}Bu$_2$C$_6$H$_3$)$_2$(THF)$_2$·THF, **1**, in high yield (eq 1).

$$^1/_2[UO_2Cl_2(THF)_2]_2 + 2KO\text{-}2,6\text{-}{}^t\!Bu_2C_6H_3 \xrightarrow{THF} \underset{\mathbf{1}}{UO_2(O\text{-}2,6\text{-}{}^t\!Bu_2C_6H_3)_2(THF)_2\cdot THF} + 2KCl \quad (1)$$

^{1}H-NMR spectra (benzene-d_6) revealed one set of resonances for the coordinated di-*tert*-butylphenoxide and one set of tetrahydrofuran multiplets. Lowering the temperature of a sample (toluene-d_8) to −60 °C did not alter the resulting

(18) Sheldrick, G. SADABS; University of Göttingen: Göttingen, Germany, 1996.
(19) Spek, A. L. *Acta Crystallogr., Sect. A* **1990**, *46*, C-34.
(20) SHELXTL, version 5.1; Bruker Analytical X-ray Systems: Madison, WI, 1997.
(21) (a) Malhotra, K. C.; Sharma, M.; Sharma, N. *Indian J. Chem., Sect. A* **1985**, *24*, 790. (b) Dua, S. K.; Kapur, V.; Sahni, S. K. *Croat. Chem. Acta* **1984**, *57*, 109..

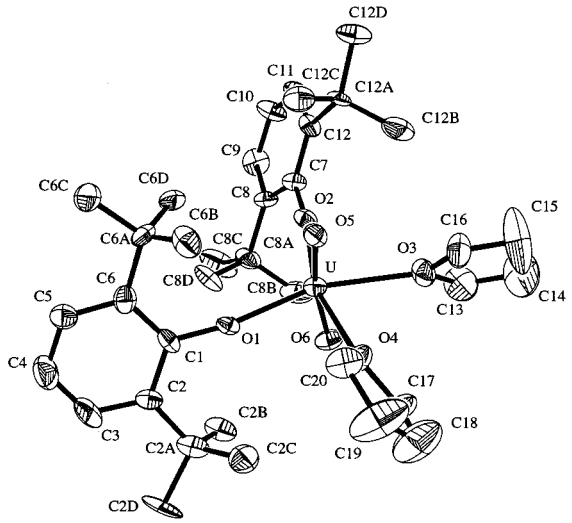

Figure 1. Molecular structure and atom-labeling scheme for UO_2(O-2,6-^{t}Bu$_2$C$_6$H$_3$)$_2$(THF)$_2$ (**1**) (50% probability ellipsoids).

spectrum, while warming the sample to 70 °C induced formation of free HO-2,6-^{t}Bu$_2$C$_6$H$_3$ and an insoluble, unidentified precipitate within hours. To determine the molecular structure of **1**, a single-crystal X-ray diffraction analysis was undertaken.

The structure determination shows that **1** exists as a monomer (Figure 1). The uranium atom is coordinated in a pseudooctahedral fashion by two apical oxo groups, two 2,6-di-*tert*-butylphenoxide ligands arranged in a cis fashion, and two THF ligands. Although the coordination of phenoxide ligands in the solid-state structure is in a cis arrangement, the possibility of a rapidly exchanging cis−trans solution equilibrium cannot be ruled out. (In fact, 77 K emission spectral data obtained in frozen tetrahydrofuran solution indicate that there are two distinct populations, vide infra.)

The oxo groups of the uranyl moiety lie trans to one another with a bond angle of 167.8(4)° (Table 2). This angle is smaller than the 174−179° angles reported for other uranyl complexes,[3b] and is probably bent in order to relieve steric strain induced between the *tert*-butyl substituents and the uranyl oxo groups. The distances between several methyl groups and appropriate -yl oxygen atoms are shorter than the sum of van der Waals radii for O^{2-} and $-CH_3$ (3.4 Å).[22] Nonbonded contacts in the structure include C(12C)−O(5) (3.312 Å), C(6D)−O(5) (3.185 Å), C(2D)−O(6) (3.338 Å), C(8B)−O(6) (3.128 Å), and C(8D)−O(6) (3.356 Å). There are a few other reports that describe uranyl compounds containing a slightly bent uranyl bond angle: [UO_2(OCH(^{i}Pr)$_2$)$_2$]$_4$, 172.6(2)°;[11b] [UO_2(H$_2$O)$_5$](ClO$_4$)$_2$·2H$_2$O, 161(3)°;[23] and (UO_2)$_3$(HO$_3$PC$_6$H$_5$)$_2$(O$_3$PC$_6$H$_5$)$_2$·H$_2$O, 174.7(2), 165.3(1), and 174.9(1)°.[9a] The U−O(oxo) distances of **1** are identical at 1.776(7) and 1.768(8) Å for O(5) and O(6), respectively. These values are comparable to those reported for six-coordinate [UO_2(OCH(^{i}Pr)$_2$)$_2$]$_4$ (1.783(4) Å),[11b] UO_2(OCHPh$_2$)$_2$(THF)$_2$ (1.779(5) Å),[11b] and UO_2(O−^{t}Bu)$_2$(OPPh$_3$)$_2$ (1.789(5), and 1.795(6) Å).[24]

The U−O(phenoxide) distances, 2.193(8) and 2.206(8) Å, are within the range of those reported for six-coordinate [Na(THF)$_3$]$_2$[UO_2(O-2,6-Me$_2$C$_6$H$_3$)$_4$] (2.217(5) and 2.190(5) Å)[13] and seven-coordinate UO_2(O-2,6-^{i}Pr$_2$C$_6$H$_3$)$_2$(py)$_3$ (2.179(5) and 2.215(5) Å).[13] The bond angles about the phenoxide oxygen atoms (173.4(7) and 169.2(7)°) are larger than those reported for other uranyl phenoxides, UO_2(O-2,6-^{i}Pr$_2$C$_6$H$_3$)$_2$(py)$_3$ (161.6(5) and 151.5(5)°)[13] and [Na(THF)$_3$]$_2$[UO_2(O-2,6-Me$_2$C$_6$H$_3$)$_4$] (159.7(5) and 167.6(5)°),[13] possibly due to steric constraints of the phenoxide ligands with the uranyl oxo groups. The U−O(tetrahydrofuran) bond lengths in **1**, 2.450(8) and 2.466(8) Å, are within range of those observed for [UO_2Cl$_2$(THF)$_2$]$_2$ (2.32(3)−2.49(4) Å).[12b,c] Other uranyl structures containing a THF ligand have U−O(THF) distances that fall within this range. The phenoxide and tetrahydrofuran ligands are each arranged in a cis geometry in the equatorial plane of the uranyl ion with O(1)−U−O(2) = 111.7(3)° and O(3)−U−O(4) = 71.9(3)°. The larger angle between the phenoxide ligands, as compared with the tetrahydrofuran ligands, is consistent with the large steric size of the di-*tert*-butylphenoxides.

For comparison against the electron-releasing properties of the di-*tert*-butyl substituents on −O-2,6-^{t}Bu$_2$C$_6$H$_3$, the coordination of a sterically bulky phenoxide, −O-2,6-Ph$_2$C$_6$H$_3$, with electron-withdrawing substituents was examined. In the latter case, the phenoxide ligands may enhance the Lewis acidic nature of the uranyl metal center. The combination of either 4 equiv of KO-2,6-Ph$_2$C$_6$H$_3$ with [UO_2Cl$_2$(THF)$_2$]$_2$ in THF at room temperature or 2 equiv of HO-2,6-Ph$_2$C$_6$H$_3$ with UO_2[N(SiMe$_3$)$_2$]$_2$(THF)$_2$ in THF at room temperature resulted in the immediate formation of an insoluble red powder (eqs 2 and 3).

$$^1/_2[UO_2Cl_2(THF)_2]_2 + 2KO\text{-}2,6\text{-}Ph_2C_6H_3 \xrightarrow{THF} \underset{\mathbf{2}}{UO_2(O\text{-}2,6\text{-}Ph_2C_6H_3)_2(THF)_2} + 2KCl \quad (2)$$

$$UO_2[N(SiMe_3)_2]_2(THF)_2 + 2HO\text{-}2,6\text{-}Ph_2C_6H_3 \xrightarrow{THF} \underset{\mathbf{2}}{UO_2(O\text{-}2,6\text{-}Ph_2C_6H_3)_2(THF)_2} + 2HNSiMe_3 \quad (3)$$

Analytically pure crystalline material was prepared by layering a hexane solution of HO-2,6-Ph$_2$C$_6$H$_3$ over a tetrahydrofuran solution of UO_2[N(SiMe$_3$)$_2$]$_2$(THF)$_2$ at room temperature. ^{1}H-NMR spectra were not obtained due to the lack of solubility of the material in the appropriate solvents. However, a single-crystal X-ray diffraction analysis of **2** was completed.

The monomeric structure of **2** is shown in Figure 2. The uranium atom lies in a pseudocentrosymmetric UO_6 coordination environment. The oxo groups of the uranyl unit lie trans to one another with a bond angle of O(1)−U(1)−O(2) = 178.4(6)°, which is within the expected range for six-coordinate uranyl.[3] The U−O bond lengths for the uranyl oxygen atoms of 1.759(14) and 1.765(12) Å are identical, and they are within the range of the U−O distances for **1**.

(22) Pauling, L. *The Nature of the Chemical Bond*, 3rd ed.; Cornell University Press: Ithaca, NY, 1960.
(23) Alcock, N. W.; Esperås, S. *J. Chem. Soc., Dalton Trans.* **1977**, 893.
(24) Burns, C. J.; Smith, D. C.; Sattelberger, A. P.; Gray, H. G. *Inorg. Chem.* **1992**, *31*, 3724.

Table 2. Selected Bond Lengths (Å) and Angles (deg) for $UO_2(O\text{-}2,6\text{-}{}^tBu_2C_6H_3)_2(THF)_2\cdot THF$ (**1**), $UO_2(O\text{-}2,6\text{-}Ph_2C_6H_3)_2(THF)_2$ (**2**), and $[UO_2(O\text{-}2,6\text{-}Cl_2C_6H_3)_2(THF)_2]_2$ (**3**)

	1		**2**		**3**	
U═O	U═O(5)	1.776(7)	U═O(1)	1.759(14)	U(1)−O(1)	1.735(11)
	U═O(6)	1.768(8)	U═O(2)	1.765(12)	U(1)−O(2)	1.743(11)
U−O	U−O(1)	2.193(8)	U−O(3)	2.209(11)	U(1)−O(3)	2.444(11)
	U−O(2)	2.206(8)	U−O(4)	2.188(11)	U(1)−O(4)	2.232(13)
	U−O(3)	2.450(8)	U−O(5)	2.413(10)	U(1)−O(3A)	2.480(11)
	U−O(4)	2.466(8)	U−O(6)	2.406(10)	U(1)−O(5)	2.461(12)
					U(1)−O(6)	2.425(12)
O−C	O(1)−C(1)	1.347(13)	O(3)−C(1)	1.368(12)	O(3)−C(1)	1.36(2)
	O(2)−C(7)	1.360(13)	O(4)−C(19)	1.375(12)	O(4)−C(7)	1.30(2)
O═U═O	O(5)−U−O(6)	167.8(4)	O(1)−U−O(2)	178.4(6)	O(1)−U(1)−O(2)	179.1(5)
U−O−C	U−O(1)−C(1)	173.4(7)	U−O(3)−C(1)	160.4(8)	U(1)−O(3)−C(1)	122.5(10)
	U−O(2)−C(7)	169.2(7)	U−O(4)−C(19)	166.8(8)	U(1)−O(4)−C(7)	177.2(13)
					U(1)−O(3A)−C(1A)	123.9(10)
U−O−U					U(1)−O(3)−U(1A)	113.6(4)

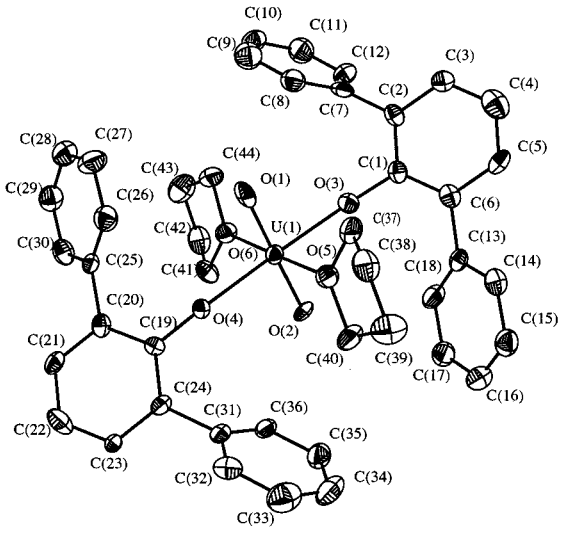

Figure 2. Molecular structure and atom-labeling scheme for $UO_2(O\text{-}2,6\text{-}Ph_2C_6H_3)_2(THF)_2$ (**2**) (50% probability ellipsoids).

In contrast to the phenoxide ligands of **1**, the two diphenylphenoxide ligands of **2** lie trans to one another. The U−O(phenoxide) distances in the molecule (U(1)−O(3) = 2.209(11) Å and U(1)−O(4) = 2.188(11) Å) are within the experimental range to those determined for **1**. The bond angles about the phenoxide oxygen atoms (U(1)−O(3)−C(1) = 160.4(8)° and U(1)−O(4)−C(19) = 166.8(8)°) are only slightly smaller than those determined for **1**, and the U−O(tetrahydrofuran) bond lengths (U(1)−O(5) = 2.413(10) Å and U(1)−O(6) = 2.406(10) Å) are shorter than those of **1**. The steric extension of the phenyl substituents may inhibit a cis geometry, although insolubility of this compound precluded investigations of cis−trans isomerization in solution. However, the structure of **2** suggests that a monomer was formed because of the steric demands of the di-*ortho*-substituted phenoxide ligands.

Additional confirmation of this hypothesis is provided by examination of the structural chemistry of uranyl phenoxide complexes with smaller substituents of variable electronegativity. The addition of 4 equiv of KO-2,6-$Cl_2C_6H_3$ to $[UO_2Cl_2(THF)_2]_2$ at room temperature in THF resulted in the formation of an orange solution (eq 4).

$$[UO_2Cl_2(THF)_2]_2 + 4KO\text{-}2,6\text{-}Cl_2C_6H_3 \xrightarrow{THF} \underset{\mathbf{3}}{[UO_2(O\text{-}2,6\text{-}Cl_2C_6H_3)_2(THF)_2]_2} + 4KCl \quad (4)$$

Analytically pure crystalline material was obtained from a tetrahydrofuran solution, layered with hexane, and cooled to −30 °C. Upon drying under a vacuum, this product becomes a powder. The ^{1}H-NMR spectrum displays only one chemical environment for the 2,6-dichlorophenoxide ligands. Lowering the temperature of the NMR sample to −60 °C did not slow this chemical exchange, while warming the NMR sample to 70 °C induced formation of free HO-2,6-$Cl_2C_6H_3$ and insoluble, unidentified precipitates after several days of heating. However, molecular weight determinations of this material in either benzene or tetrahyrofuran indicate the existence of a dimer, $[UO_2(O\text{-}2,6\text{-}Cl_2C_6H_3)_2(THF)_2]_2$.[25,26]

A single-crystal X-ray diffraction analysis of **3** was undertaken. As expected, the compound exists as a dimer (Figure 3). The molecule has an inversion center in the equatorial plane between the two parallel uranyl units, and each uranium is coordinated in a pseudopentagonal bipyramidal geometry by seven oxygen atoms. The ring planes of the phenoxide and tetrahydrofuran ligands lie perpendicular to the equatorial plane of the uranyl groups. The uranium atoms are bridged by two 2,6-dichlorophenoxide ligands, and a terminal 2,6-dichlorophenoxide group is coordinated to each uranium. Two tetrahydrofuran ligands are also coordinated to each uranium in a nonadjacent fashion.

The oxo groups of the uranyl moiety lie trans to one another with a near linear O═U═O bond angle of 179.1(5)°, as is commonly found for structures of uranyl complexes. The U−O(oxo) distances at 1.735(11) and 1.743(11) Å are identical within experimental error. These values are consistent with U−O distances found in seven-coordinate uranyl complexes $UO_2(O\text{-}2,6\text{-}{}^iPr_2C_6H_3)_2(py)_3$ (1.785(5) and 1.792(5) Å)[13] and $[UO_2Cl_2(THF)_2]_2$ (1.76(3) and 1.74(2) Å).[12b,c]

(25) The molecular weight of **3** was determined using a molecular weight apparatus.[27] Weight determined in benzene: 1478 amu. Weight determined in tetrahydrofuran: 1461 amu. Expected molecular weight for dimer: 1476.40 amu.

(26) Zoellner, R. W. *J. Chem. Educ.* **1990**, *67*, 714.

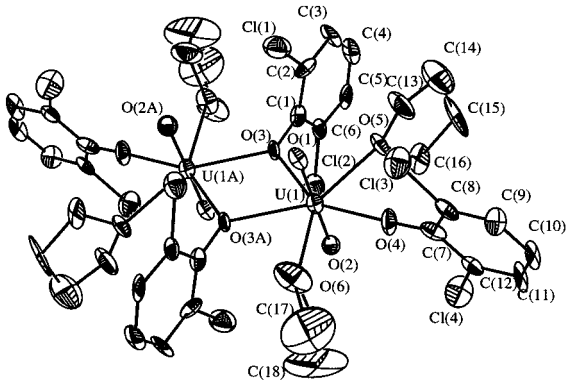

Figure 3. Molecular structure and atom-labeling scheme for $[UO_2(O\text{-}2,6\text{-}Cl_2C_6H_3)_2(THF)_2]_2$ (**3**) (50% probability ellipsoids).

The U−O(phenoxide$_{terminal}$) bond (2.232(13) Å) is longer than those reported for six-coordinate **1** and **2**, as would be expected with consideration of the larger coordination number. The value in **3** is the same within error of U−O(phenoxide$_{terminal}$) for seven-coordinate $UO_2(O\text{-}2,6\text{-}{}^{i}Pr_2C_6H_3)_2(py)_3$ (2.179(5) and 2.215(5) Å).[13] The U−(μ-O) bond distances are slightly asymmetric (U(1)−O(3) = 2.444(11) Å and U(1)−O(3A) = 2.480(11) Å). The bond angles about the terminal phenoxide oxygen atoms (U−O(4)−C(7), 177.2(13)°) are near linear, and the U−O−C bond angles about the bridging phenoxide oxygen atoms (U(1)−O(3)−C(1), 122.5(10)°; U(1)−O(3A)−C(1A), 123.9(10)°) are bent more due to the more constrained environment surrounding these bridging phenoxide ligands. U−O(THF) distances to the tetrahydrofuran ligands in **3** (2.461(12) and 2.425(12) Å) are similar to those found in **1** and **2**. The dimeric geometry of **3** is also comparable to the structure of $[UO_2Cl_2(THF)_2]_2$, in which each uranium is coordinated in a pseudopentagonal bipyramidal fashion by two apical oxo groups, one terminal chloride, two bridging chloride ions, and two nonadjacent THF ligands.[12b,c]

A comparison of the six-coordinate geometries surrounding the uranium atoms of **1** and **2** with the seven-coordinate environments of the uranium atoms in **3** also suggests that the steric properties of the ligand manifest themselves in the resultant structure of the molecule.[27] The large sizes of the 2,6-di-*tert*-butylphenoxide and 2,6-diphenylphenoxide ligands allow for a six-coordinate geometry around the uranium atoms of **1** and **2**, rather than a seven-coordinate geometry found for **3**. To verify that the steric demands of the substituted phenoxide ligand are more influential on the product structure than the electronic properties, we attempted to synthesize a uranyl compound coordinated by a less sterically demanding phenoxide (2,6-dimethylphenoxide). The reaction of 4 equiv of KO-2,6-$Me_2C_6H_3$ with $[UO_2Cl_2(THF)_2]_2$ in THF gave a crystalline product (eq 5) which was difficult to separate from KCl. However, low-temperature recrystallization from a THF/hexane solution allowed for the isolation of dark red-black blocks.

$$[UO_2Cl_2(THF)_2]_2 + 4KO\text{-}2,6\text{-}Me_2C_6H_3 \xrightarrow{THF} \underset{\mathbf{4}}{[UO_2Cl(O\text{-}2,6\text{-}Me_2C_6H_3)(THF)_2]_2} + 2KCl \quad (5)$$

Analysis by ^{1}H-NMR was thwarted by poor solubility in hydrocarbon solvents.

Multiple sets of X-ray data collected for the crystals of **4** show that the crystals are severely twinned and allow only the atom connectivity within the molecule to be determined; no further structural information will be presented (see deposited material). Compound **4** is a dimer, analogous to the structure of **3** and $[UO_2Cl_2(THF)_2]_2$ (Figure 4).[12b,c] Each uranium is coordinated by seven atoms in a pseudopentagonal bipyramical geometry, with oxygen atoms in the apical positions. The uranium atoms are bridged by phenoxide ligands, and each uranium atoms has one terminal chloride ion and two THF ligands coordinated in the equatorial plane. The apparent dimeric structure of this compound indicates that the structural type of uranyl phenoxide complex (monomer vs dimer) is clearly correlated with the steric requirements of the phenoxide rather than the electronic contributions. Furthermore, elemental analysis of the bulk material reveals a stoichiometry consistent with $UO_2Cl_{1.2}(O\text{-}2,6\text{-}Me_2C_6H_3)_{0.8}(THF)_2$, the possible result of an incomplete metathesis.

Spectroscopic Characterization. Additional information on molecular and electronic structural variations in compounds containing the uranyl chromophore can frequently be provided by the examination of electronic (absorption and emission) and vibrational (infrared and Raman) spectroscopic data. These methods have been routinely used to determine the speciation of uranyl-bearing species in aqueous environments,[5b,28] and trends have begun to emerge relating spectroscopic data, molecular structural characteristics, and ligand properties. In particular, the influence of basicity of the equatorial ligands on the energy of the lowest-lying electronic transition and the energy of the totally symmetric uranyl stretching vibration has been explored in some detail.[29,30] There are a few recent reports characterizing the spectral trends for uranyl species as they undergo successively greater extents of oligomerization (monomers, dimers, etc.).[28b−e] The theoretical underpinnings for some of these relationships between molecular and electronic structure have been addressed and provide a platform for initial interpretation of

(27) Leciejewicz, J.; Alcock, N. W.; Kemp, T. J. *Struct. Bonding (Berlin)***1995**, *82*, 43.

(28) (a) Clark, D. L.; Conradson, S. D.; Donohoe, R. J.; Keogh, D. W.; Morris, D. E.; Palmer, P. D.; Rogers, R. D.; Tait, C. D. *Inorg. Chem.* **1999**, *38*, 1456. (b) Kitamura, A.; Yamamura, T.; Hase, H.; Yamamoto, T.; Moriyama, H. *Radiochim. Acta* **1998**, *82*, 147. (c) Moulin, C.; Laszak, I.; Moulin, V.; Tondre, C. *Appl. Spectrosc.* **1998**, *52*, 528. (d) Meinrath, G.; Kato, Y.; Kimura, T.; Yoshida, Z. *Radiochim. Acta* **1998**, *82*, 115. (e) Meinrath, G. *J. Radioanal. Nucl. Chem.* **1997**, *224*, 119. (f) Bernhard, G.; Geipel, G.; Brendler, V.; Nitsche, H. *Radiochim. Acta* **1996**, *74*, 87. (g) Moulin, C.; Decambox, P.; Moulin, V.; Decaillon, J. G. *Anal. Chem.* **1995**, *67*, 348. (h) Kato, Y.; Meinrath, G.; Kimura, T.; Yoshida, Z. *Radiochim. Acta* **1994**, *64*, 107. (i) Morris, D. E.; Chisholm-Brause, C. J.; Barr, M. E.; Conradson, S. D.; Eller, P. G. *Geochim. Cosmochim. Acta* **1994**, *58*, 3613. (j) Nguyen-Trung, C.; Begun, G. M.; Palmer, D. A. *Inorg. Chem.* **1992**, *31*, 5280.

(29) Denning, R. G. *Struct. Bonding (Berlin)* **1992**, *79*, 215.

(30) McGlynn, S. P.; Smith, J. K.; Neely, W. C. *J. Chem. Phys.* **1961**, *35*, 105.

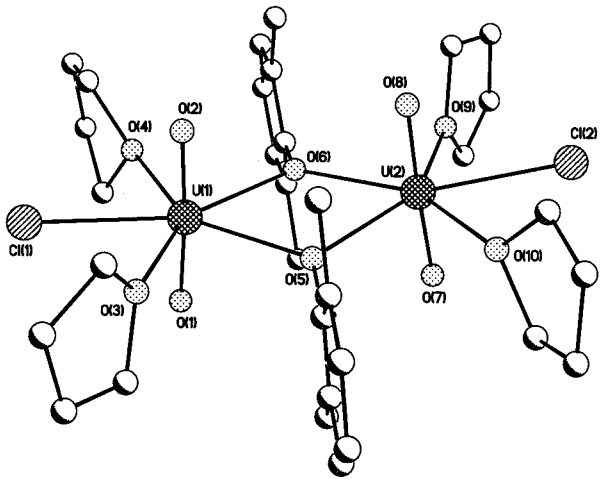

Figure 4. Molecular structure and atom-labeling scheme for $[UO_2Cl(O\text{-}2,6\text{-}Me_2C_6H_3)(THF)_2]_2$ (**4**).

results.[29] A spectroscopic investigation of the aryloxide complexes reported here was undertaken with two principal goals: (1) to look for evidence of equilibrium processes (monomer/multimer and *cis*-/*trans*-isomer) in solution similar to that observed previously in the $[UO_2(OCH(^iPr)_2)_2]_4$ system[11b] and (2) to compare the ligand basicity/excited-state electronic energy relationship in these aryloxide complexes with those observed in other uranyl coordination compounds.

One of the initial considerations in this investigation was to search for evidence of solution equilibria between monomeric and dimeric species and cis−trans conformers of the monomeric species for these aryloxide complexes. The single-crystal X-ray data clearly reveal a preference in the solid state for a dimeric complex with the sterically less encumbered phenoxide ligands (2,6-dichlorophenoxide and 2,6-dimethylphenoxide), whereas the sterically demanding ligands, 2,6-di-*tert*-butylphenoxide and 2,6-diphenylphenoxide, give rise to monomeric solid complexes having cis and trans ligand conformations, respectively. As previously noted, variable-temperature ^{1}H-NMR data for the solutions of these complexes (except for **2**) are ambiguous with respect to both monomer/dimer equilibria and the cis−trans isomerization processes. However, we have shown previously that luminescence spectroscopy at ∼77 K is an excellent diagnostic for equilibrium mixtures of species in frozen solutions.[11b,28a] In particular, we have recently demonstrated that the tetrameric solid complex $[UO_2(OCH)(^iPr)_2]_4$ undergoes a deaggregation reaction in coordinating solvents, such as tetrahydrofuran, to give mixtures of what are proposed to be monomeric and dimeric species in solution.[11b]

Low-temperature luminescence data for **3** in tetrahydrofuran at 0.1, 1.0, and 10 mM with respect to the dimeric starting complex are shown in Figure 5. The spectrum of the most-dilute solution (A) shows clear evidence for two populations of species. One dominates the spectrum at the two higher concentrations, shown in B and C. The second population is seen in the spectrum of A as a shoulder on the high-energy side of the first prominent vibronic band and filling between each of the other vibronic bands of the dominant spectral constituent. The result of the spectral

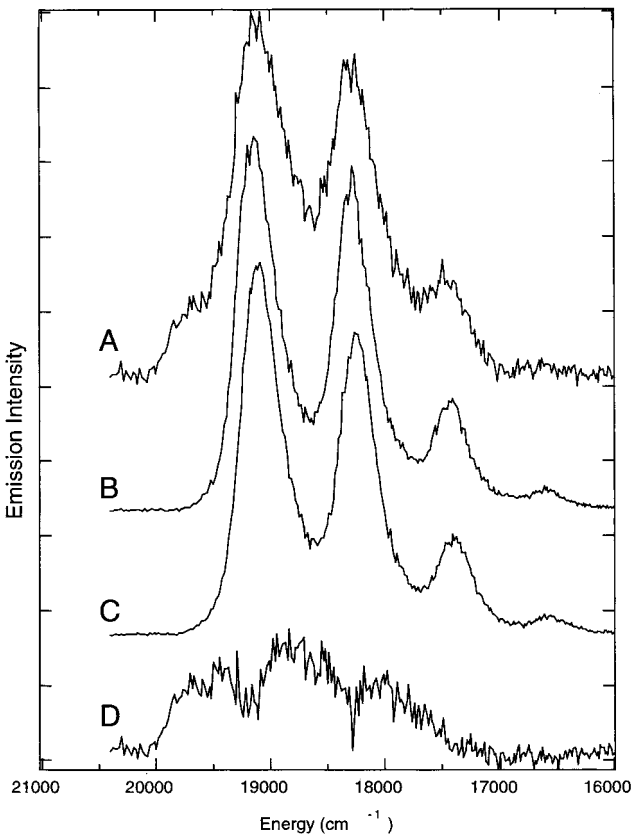

Figure 5. Electronic emission spectra of tetrahydrofuran solutions of $[UO_2(O\text{-}2,6\text{-}Cl_2C_6H_3)_2(THF)_2]_2$ (**3**) at (A) 0.1 mM, (B) 1.0 mM, and (C) 10 mM. Spectrum D represents the deconvolution of spectrum A to isolate the spectrum of the second component in this solution. Spectra were obtained at the liquid nitrogen temperature.

deconvolution to obtain a clearer representation of the spectrum of this second, higher-energy emission component is seen in the most-dilute sample (D). This difference spectrum suffers from a poor signal/noise ratio (derived from the more dilute parent spectrum), but it does show vibronic resolution and a higher-energy electronic origin energy [31] than that seen in the spectrum at the higher solution concentrations. The disappearance of this weaker, higher-energy spectral component with increasing concentration of the complex is consistent with a solution equilibrium between uranyl species. The dependence on the total uranium concentration suggests that the equilibrium involves species that differ in the number of uranyl moieties per species.

The simplest explanation of this behavior is a monomer−dimer equilibrium, with the dimeric form dominating the equilibrium at all but the most-dilute concentration. The assignments of the difference spectrum (Figure 5, spectrum D) to a monomeric complex and the principal constituent in the higher-concentration spectra (B, C) to a dimeric complex of the dichlorophenoxide ligand are consistent with spectral

(31) The exact location of the electronic origin (E_{0-0}) is frequently difficult to discern in uranyl spectra at the level of resolution obtained here. In particular, for systems with a rigorous inversion symmetry, the 0−0 transition is electric-dipole forbidden, and the highest-energy emission feature frequently arises in a vibronic transition one quantum lower in energy than the true E_{0-0}. Here we report apparent E_{0-0} values based on the calculation of the first observed vibronic band. The exact position of the electronic origin could lie to higher energy.

Table 3. pK_a Values for Corresponding Phenols,[32] Spectroscopic Data, and Key Bond Lengths for Compounds **1**, **2**, **3**, and **4**

	1	**2**	**3**	**4**
di-*ortho*-phenoxide	O-2,6-^{t}Bu$_2$C$_6$H$_3$	O-2,6-Ph$_2$C$_6$H$_3$	O-2,6-Cl$_2$C$_6$H$_3$	O-2,6-Me$_2$C$_6$H$_3$
pK_a	11.7	<10.01	6.79	10.6
E_{0-0} dimer, cm^{-1}	N/A	N/A	19 100	20 100
E_{0-0} monomer, cm^{-1}	19 050	19 290	19 500	19 300
ν_1, cm^{-1}	804	808	839	835
U═O	1.768, 1.776	1.759, 1.765	1.735, 1.743	
U═O average	1.772	1.762	1.739	
U−O	2.193, 2.206	2.188, 2.209	2.232	
U−O average	2.2	2.199	2.232	
U−μ−O			2.444, 2.480	
U−μ−O average			2.462	
U−THF	2.450, 2.466	2.406, 2.413	2.425, 2.461	
U−THF average	2.458	2.41	2.443	

trends seen for other uranyl oligomers. Specifically, the spectrum of the monomeric solvated uranyl species in aqueous solution, $[UO_2(OH_2)_5^{2+}]$, lies with a slightly higher energy than that of the simplest dimeric hydrolysis species, $[UO_2(OH)(OH_2)_3]_2^{2+}$.[28b] Similarly, for the novel tetrameric uranyl alkoxide noted above,[11b] the spectrum of the putative dimeric deaggregation product in THF solution is shifted to a higher energy than that of the intact tetramer, and the spectrum of the proposed monomeric product is shifted to a higher energy than that of the dimer. The magnitude of the spectral shift between monomeric and dimeric forms for **3** (~300 cm^{-1}, Figure 5) is comparable to the shift observed between the aqueous monomeric and dimeric hydrolysis species (~210 cm^{-1})[28b] but much less than that observed between the monomeric and dimeric deaggregation products of the di-*iso*-propylmethoxide tetramer (~1800 cm^{-1}).[11b] A monomer−dimer equilibrium for the system of **3** would mimic the deaggregation of this tetrameric species. The free tetrahydrofuran is likely to occupy an additional equatorial coordination site to satisfy the 5-fold equatorial coordination found in the dimeric structure (eq 6).

$$\underset{\mathbf{3}}{[UO_2(O\text{-}2,6\text{-}Cl_2C_6H_3)_2(THF)_2]_2} + 2THF \rightarrow 2UO_2(O\text{-}2,6\text{-}Cl_2C_6H_3)_2(THF)_3 \quad (6)$$

A less pronounced concentration dependence is also observed in the ~77 K luminescence spectral behavior of **4** (a dimer in the solid state) and **1** (a *cis*-monomer in the solid state). The data for **4** are comprised of spectral signatures from two species whose relative contributions to the net spectra change with total uranium concentration. However, for this system, the spectral component of the species that dominates the spectrum at the higher concentration is shifted to a *higher* energy than that of the species dominating at the dilute concentrations (i.e., the opposite of what is observed for the system of **3**). However, results from elemental analysis suggest that there is a substoichiometric amount of the 2,6-dimethylphenoxide ligand present in the bulk isolated product, even upon successive recrystallizations. The inhomogeneous excess of the coordinated chloride ion could account for the observed spectral behavior from low to high uranium concentration noted above. For **1**, there are insufficient data as a function of complex concentration to deduce clear trends. For **2**, there are no solution emission data that could be obtained due to the insolubility of this complex in all the solvents tested.

The second goal of this spectral investigation is to assess the influence of the basicity of the equatorial aryloxide ligands on the electronic excited-state energy in these complexes, particularly in comparison to other uranyl coordination compounds. Previous work has led to a well-established trend of decreasing electronic origin energy (E_{0-0}) and decreasing U═O vibrational energies with increasing equatorial ligand basicity.[29,30] The spectral data for these aryloxide complexes are summarized in Table 3. As noted above, the ligand basicity increases for the complexes considered here as dichlorophenoxide < diphenylphenoxide < dimethylphenoxide < di-*tert*-butylphenoxide.[32]

A comparison of the ~77 K luminescence data for the dominant form (i.e., the species isolated as the solid product) of the four complexes under consideration reveals no real trend in the electronic origin energy of the spectra for the complexes of these ligands (Figure 6). In fact, there are only minimal differences in the electronic origin energies of **1**−**3**. The spectrum of **4** appears to be an outlier in this comparison, but as noted above, terminal chloride complexation could have a significantly different perturbing influence on the electronic energy in this complex. If one ignores the data from **4** and compares spectra from only the species postulated to be monomeric (Figures 5D and 6), there is a decrease in emission energy with increasing ligand basicity (Table 3).

The vibrational spectroscopic data (infrared and Raman) for solid samples of all four aryloxide complexes are shown in Figure 7. The totally symmetric uranyl stretch is anticipated to be the most intense mode in the Raman spectra due to its intrinsic polarizability, and generally, good agreement is obtained between the ν_1 Raman band assigned on this basis and the value derived from the vibronic progression spacing in the emission spectra. Totally unambiguous assignments would require isotopic labeling and polarization measurements that are beyond the scope of the present study. Comparison of the vibrational energies for the ν_1 uranyl modes for **1**−**3** (Table 3) does show the anticipated decrease in energy with increasing ligand basicity.

Perhaps the most notable observation from these spectral data for the aryloxide complexes is that they appear to define

(32) Serjeant, E. P.; Dempsey, B. In *Ionisation Constants of Organic Acids in Aqueous Solution*; Pergamon Press: New York, 1979.

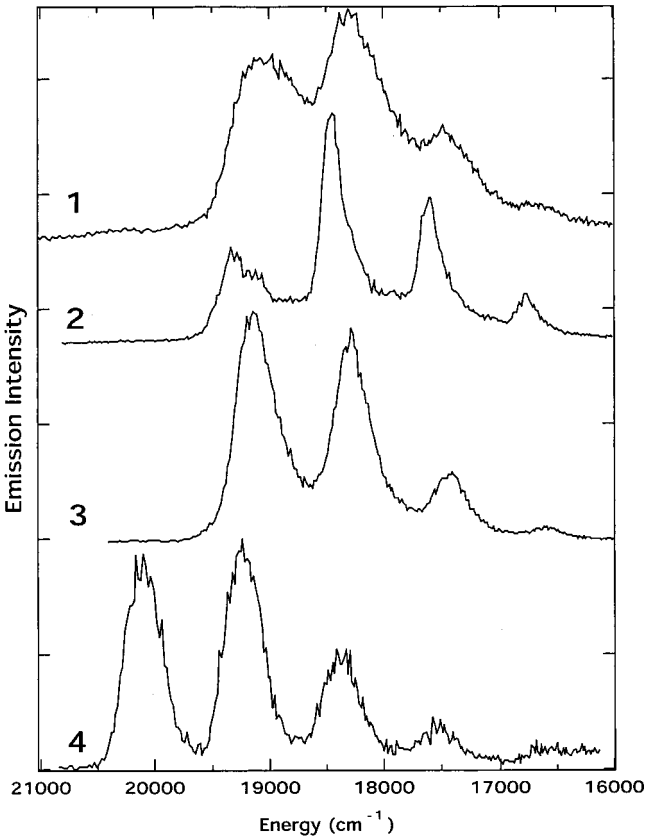

Figure 6. Electronic emission spectra of solid compounds UO_2(O-2,6-^{t}-$Bu_2C_6H_3)_2(THF)_2$·THF (**1**), UO_2(O-2,6-$Ph_2C_6H_3)_2(THF)_2$ (**2**), [UO_2(O-2,6-$Cl_2C_6H_3)_2(THF)_2]_2$ (**3**), and [UO_2Cl(O-2,6-$Me_2C_6H_3$)$(THF)_2]_2$ (**4**). Spectra were obtained at the liquid nitrogen temperature.

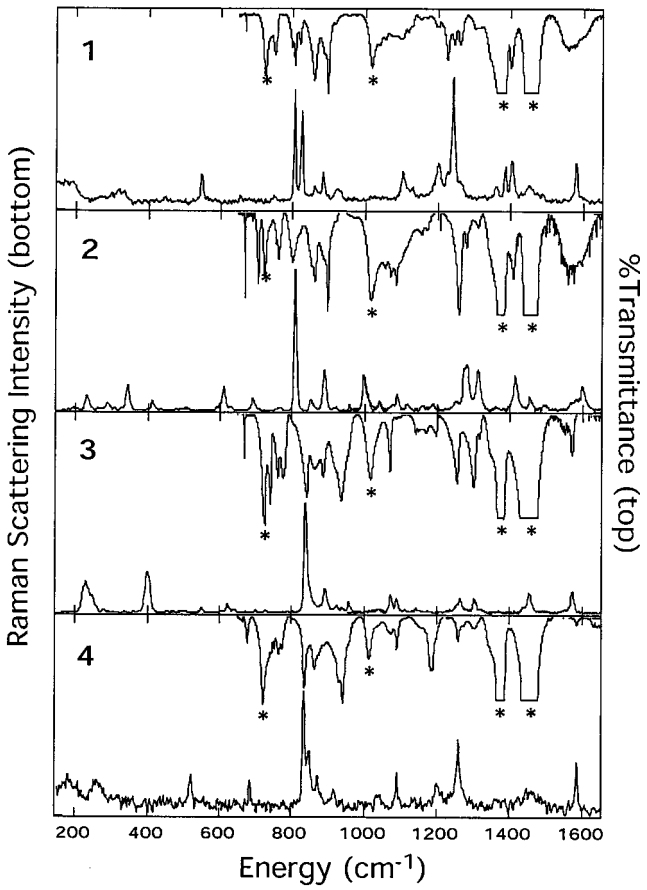

Figure 7. Infrared spectra (upper) and Raman spectra (lower) for UO_2(O-2,6-^{t}-$Bu_2C_6H_3)_2(THF)_2$·THF (**1**), UO_2(O-2,6-$Ph_2C_6H_3)_2(THF)_2$ (**2**), [UO_2-(O-2,6-$Cl_2C_6H_3)_2(THF)_2]_2$ (**3**), and [UO_2Cl(O-2,6-$Me_2C_6H_3$) $(THF)_2]_2$ (**4**) in the solid state. All Raman solids were run neat, except for the sample of **1**, which was diluted in a 1:10 ratio in spectroscopic grade KBr. Asterisks in IR data indicate bands from Nujol mull.

a completely different class of uranyl chromophores relative to the more classical uranyl coordination compounds. For example, a reasonably good linear relationship is observed between the U═O bond length and the electronic origin energy for 16 uranyl coordination compounds in ref 29 (Figure 21), and this relationship correlates well with the basicity of the equatorial ligands. However, if the U═O bond length/electronic origin energy data points for these aryloxide complexes are compared with those in ref 29, one finds that the points define a completely different population. The electronic origin energies are comparable to those for the most-basic coordination compound ligands (e.g., the uranate salts that possess all oxo ligands), yet the U═O bond lengths for these aryloxide complexes are commensurate with those of much less-basic equatorial ligand coordination compounds, such as those of acetato ligands. This likely reflects the interplay between the strong σ-donor capability of the aryloxide ligands and their steric encumberance that inhibits the full impact of the electron-donating ability of these ligands on the electronic and molecular structural properties.

Conclusions

Metathesis reactions of uranyl chloride with di-*ortho*-substituted phenoxides have been found to yield either monomeric or dimeric uranyl phenoxide products. Reactions of [$UO_2Cl_2(THF)_2]_2$ with KO-2,6-^{t}$Bu_2C_6H_3$ or KO-2,6-$Ph_2C_6H_3$ result in the formation of monomeric compounds *cis*-UO_2(O-2,6-^{t}$Bu_2C_6H_3)_2(THF)_2$·THF, **1**, and *trans*-UO_2(O-2,6-$Ph_2C_6H_3)_2(THF)_2$, **2**. Compound **2** may also be prepared from an alcoholysis reaction between $UO_2[N(SiMe_3)_2]_2$-$(THF)_2$ and 2 equiv of HO-2,6-$Ph_2C_6H_3$. The reaction of [$UO_2Cl_2(THF)_2]_2$ with 4 equiv of KO-2,6-$Cl_2C_6H_3$ is found to produce the dimeric compound [UO_2(O-2,6-$Cl_2C_6H_3)_2$-$(THF)_2]_2$, **3**. Furthermore, the incomplete metathesis of [UO_2-$Cl_2(THF)_2]_2$ with KO-2,6-$Me_2C_6H_3$ allows for the formation of dimeric [UO_2Cl(O-2,6-$Me_2C_6H_3$)$(THF)_2]_2$, **4**.

While these results obviously do not indicate any change in the structure of the uranyl moiety itself, this study illustrates that simple aggregation of uranyl is principally influenced by the steric size of the substituents on the aryloxide ligands. Furthermore, emission and vibrational data support the conclusion that the steric demand of the equatorial ligands is the principal determinant in defining the most-stable molecular structure. Spectroscopic evidence suggests that the innate electron-donating capacity of the ligands is only subtly manifest in the electronic or vibrational energy distributions within these molecules. We are presently engaged in attempts to synthesize other uranyl compounds containing a variety of other coordinated electron-donating alkoxides (OR; R = alkyl). We predict that uranyl aggregates

containing more electron-donating alkoxide ligands may be capable of forming structures resulting from Lewis basic oxo groups.

Acknowledgment. This research was supported by the Division of Chemical Energy Science, Office of Basic Energy Sciences, U.S. Department of Energy, and by the Los Alamos National Laboratory Directed Research and Development Program. Los Alamos National Laboratory is operated by the University of California for the U.S. Deparment of Energy under Contract W-7405-ENG-36.

Supporting Information Available: X-ray crystallographic files, in CIF format, for **1**−**3**. This material is available free of charge via the Internet at http://pubs.acs.org.

IC011080Q